JOURNAL OF PROPULSION AND POWER
Vol. 17, No. 2, March–April 2001

Direct Evidence of Spatial Burning Rate Variation as Cause of Midweb Anomaly

Desh Deepak,* R. Jeenu,† P. Sridharan,† and M. S. Padmanabhan‡
Vikram Sarabhai Space Centre, Thiruvananthapuram 695 022, India

With the use of the ultrasonic pulse-echo technique, local burning rates are measured at different radial locations across the web during static tests of center-perforated solid propellant rocket motor grains. The measurement shows a higher burning rate in the midweb region and a lower burning rate toward the port and motor case. The measured motor pressure history could be very well simulated by using the measured local burning rates. Thus, direct evidence is provided that the variation of the burning rate across the web is the cause of the midweb anomaly in chamber pressure widely reported in solid motors with center-perforated grains.

Nomenclature

a = constant
C = acoustic velocity
K = constant
n = burning-rate index
p = pressure
r = burning rate
T = temperature
x = thickness
Δt = time lapse

Subscripts

AN = web-average normalized
L = local
LN = local normalized
m = measured
p = pressure
ref = reference
T = temperature

Introduction

FOR solid rocket motors with low port flow velocities, the prediction of pressure or thrust–time history considers burning rate as a function of pressure (e.g., $r = ap^n$), but the burning-rate parameters are assumed to be independent of web location. However, in motor tests of center-perforated composite solid propellant grains, the measured pressure history often differs from the pressure–time curve so predicted, though by a small magnitude.[1–3] This deviation in pressure (usually, a lower pressure than predicted in the initial and final portions of the web, and a higher pressure than predicted in the midweb portion of the grain) is variously termed "midweb anomaly," "hump factor," "burning anomaly rate factor," and so on. The midweb anomaly has been observed both in subscale and full-scale solid rocket motor firings, with star grains as well as cylindrical grains. The typical magnitude of an anomaly in motor pressure is in the range 0–6%.

Various studies have attributed the midweb anomaly primarily to spatial variations in the local burning rate within the propellant grain, as a result of rheological processes involved in the flow of propellant slurry between the mandrel and the case wall during motor casting. The role of rheological processes in midweb anomaly was observed by Kallmeyer and Sayer,[1] who noted distinct changes in the pressure–time curve of the Space Shuttle solid rocket booster (SRB) when the forward and center segment casting arrangement was modified between the development and qualification programs. Studies by Beckman and Geisler[2] showed a decrease in the extent of anomaly with an increase in oxidizer particle size ratio (coarse/fine), whereas no influence of aluminum content in the propellant was observed. Friedlander and Jordan[3] hypothesized that the burning-rate variation is due to the variation in local propellant composition as a result of striation of the binder-rich layers of the propellant in the high shear regions during casting. Also, it has been noted that the gradients of shear forces in propellant flow during casting may result in preferential orientation, or alignment of larger oxidizer particles.[4] The dependence of burning rate on oxidizer particle orientation is supported by various investigations.[4,5] Neilson and Miles[6] observed that the high pressures obtained during the early portion of several SRB firings were caused by changes in the size/shape characteristics of the ammonium perchlorate particles, which might also be explained by the particle alignment scenario.

In all the above studies except Ref. 3, the burning-rate variation across the web was not measured, but was inferred from the observed pressure–time pattern. In Ref. 3 as well as in a few other investigations,[6,7] measurement has been made of burning rate, but this has been done on strands cut from different locations in the grain. However, no investigation has been reported where the midweb anomaly in pressure is demonstrated to be due to variation of burning rates from direct measurement within the grain as the burning proceeds.

In the present work, local burning rates are measured at different radial locations in the web during motor firings of center-perforated propellant grains, using the nonintrusive ultrasonic technique. After normalization to a reference pressure to remove the pressure effect, the burning rates are observed to be higher in the midweb region and lower toward the port and case. A clear pattern in burning rate is seen in repeated firings. The motor pressures predicted by using the local burning rates are in excellent agreement with the measured pressure vs time history of the motor, including in the midweb region. Thus, this study gives direct evidence of the variation of burning rate of propellant in the web of the motor grain as the cause for the observed midweb anomaly in solid propellant motors.

Experimental Details

Ultrasonic Pulse-Echo Technique

The burning-rate measurements were made by using the nonintrusive ultrasonic pulse-echo technique during the firings of ballistic evaluation motors (BEMs). The ultrasonic technique used the Pulse-Echo Interface Measurement (PIM) system[8,9] developed by

Received 2 June 1999; revision received 30 March 2000; accepted for publication 27 June 2000.

*Section Head, Combustion R&D Section, Fluid Mechanics and Internal Ballistics Division.
†Scientist/Engineer, Fluid Mechanics and Internal Ballistics Division; P. Sridharan is currently in the Advanced Propulsion Facility Division.
‡Division Head, Fluid Mechanics and Internal Ballistics Division.

TNO-Prins Maurits Laboratory, The Netherlands. It involves the transmitting of an ultrasonic pulse through the propellant grain web and the reception of the reflected echo pulse from the burning surface–combustion gas interface by the same transducer.[9–12] The pulses through the transducer can be emitted at an adjustable rate of 0.5–5 kHz. The PIM system measures the time lapse between the emitted and received pulses during the propellant burning. From this, the instantaneous web thickness, x, of the burning propellant is obtained from the relation

$$x = C\Delta t/2 \tag{1}$$

The burning rate at any instant is determined from the web thickness vs time data, that is, $r = -\mathrm{d}x/\mathrm{d}t$. In Eq. (1), the acoustic velocity, C, is given by

$$C/C_{\mathrm{ref}} = [1 + K_T(T - T_{\mathrm{ref}})][1 + K_p(p - p_{\mathrm{ref}})] \tag{2}$$

where K_T and K_p are constants for a particular propellant. The procedure for evaluating K_T and K_p is discussed elsewhere.[12] The reference condition, in the above context, is the ambient temperature and ambient pressure.

A coupling material, for example, poly (methyl methacrylate), or PMMA, is used between the propellant and the ultrasonic transducer to isolate the transducer from the severe pressure and temperature conditions in the motor chamber. Also, the coupling element reduces the near-field effect of the ultrasonic transducer and allows the operation of the technique down to low propellant thicknesses.

Accuracy of Burning-Rate Measurements

The accuracy and repeatability of measurements by the ultrasonic technique were established[12] by measuring the burning rate of end-burning propellant specimens (diameter of 30 mm and length of 30 mm) at a nearly constant pressure. The measured burning rates for four tests normalized to 3.24 MPa (33 kgf/cm^2) are given in Table 1. This shows that the burning-rate values are consistent and are within ±1%. From the same propellant mix, two motor grains were prepared and the motors were static tested. The burning rates were evaluated in the two motor tests by the conventional method (ratio of the web thickness to the burn time of the motor). The burning rate at 3.24 MPa was 4.96 mm/s in motor No. 1, and 4.97 mm/s in motor No. 2. This further confirms the results obtained by the use of the ultrasonic technique.

Table 1 Results of burning-rate measurements of propellant specimens, using the ultrasonic technique

Test No.	Normalized burning rate at 3.24 MPa (mm/s)	Maximum variation during a test (%)
1	4.92	0.04
2	4.94	0.90
3	4.96	1.06
4	4.95	0.66

Ballistic Evaluation Motor

The BEM had a diameter of ~200 mm with an ~1000 mm long cylindrical port grain designed to give the chamber pressure variation from 2.5 to 4.5 MPa during its burning time of ~6 s. The weight of propellant grain was ~31 kg. The grain dimensions (in millimeters) are as follows: length, 970; o.d. at head end, 196; i.d. at head end, 120; o.d. at nozzle end, 197; i.d. at nozzle end, 133. The nozzle throat diameter was 52.5 mm. Details of the motor are shown in Fig. 1. As a way to avoid any erosive burning component, burning-rate measurements were made at the head end of the grain. For this purpose, the mild steel motor case had a cut out at the head-end side of the motor chamber to fix the premachined PMMA coupling element. The motor case was insulated except at the location of the PMMA, so that the outer diameter of the propellant grain at this location was in direct contact with the PMMA coupling element.

Propellant Grain

The propellant was of aluminized composite type (AP-HTPB-Al; 18% Al, 86% solid loading), cast in the insulated motor chamber with the cylindrical mandrel in place. The propellant casting arrangement is shown in Fig. 2. Ground and sieved ammonium perchlorate particles of average sizes of 300 and 40 μm in a ratio of

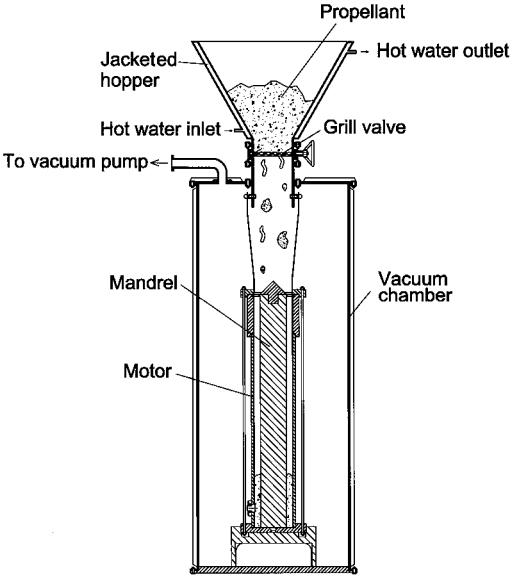

Fig. 2 Setup for the propellant casting in the motor.

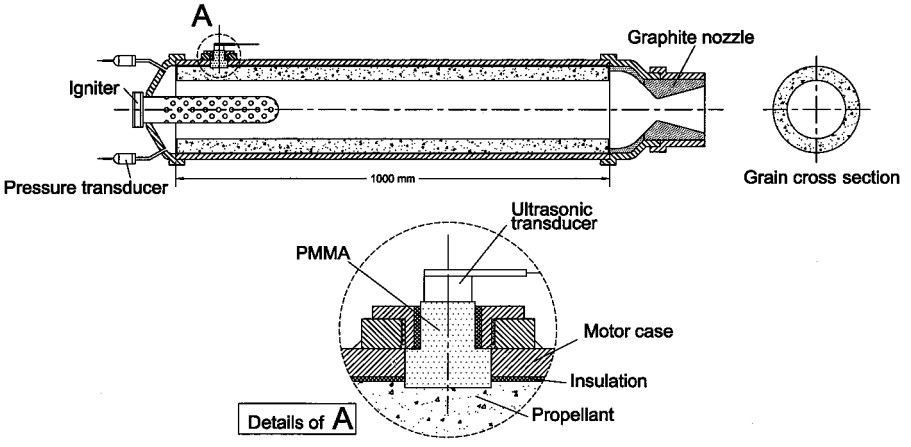

Fig. 1 Schematic of the ballistic evaluation motor for burning-rate measurements by use of the ultrasonic technique.

3:1 were used for the propellant preparation. The average size of the aluminium particles was 15 μm. The ingredients of the propellant were mixed in a horizontal sigma blade kneader, and the propellant was vacuum cast in the motor chamber with the propellant slurry flowing through a grill plate over the mandrel into the annulus between the mandrel and the wall of the motor chamber. The cast motors were cured at a constant temperature in an oven. After curing, the mandrel was removed and both the ends of the propellant grain were trimmed and inhibited. The head end and nozzle were assembled for the static firing of the motors.

Instrumentation and Static Test

During motor firing, the motor pressure and burning rate of the propellant were measured. For the burning rate to be measured, an ultrasonic transducer connected to the PIM system was mounted on the PMMA coupling element at the head end of the motor. A heavily damped, broadband ultrasonic transducer operating at a frequency of 2.25 MHz and with an element size of 13 mm was used for this study. The PIM system was operated for ultrasonic pulse emission frequency of 2000 pulses/s. Pressure at the head end of the motor was measured by pressure transducers. The outputs of the PIM system and the pressure transducer were recorded at the rate of 500 pieces of data/s by using a personal-computer-based data-acquisition system. Four static motor tests were conducted. The results of these static tests are discussed in the next section.

Results and Discussion

The web thickness of propellant grain measured by the PIM system and the motor pressure in a static test of BEM are shown in Fig. 3. The measured pressure history shows the classic hump pattern in the midweb region. This behavior in motor pressure was observed in all four motor tests conducted. When the test data are analyzed, the ignition and tailoff transients are excluded; only the measurements in steady state are considered. From the web burnt vs time data, the local burning rates (r_L) across the web were determined for a time increment of 0.3 s. As a way to account for the pressure effect, the local burning rates were normalized to a reference pressure ($p_{\text{ref}} = 3.24$ MPa), using the burning-rate law, $r = ap^n$. Thus,

$$r_{\text{LN}} = r_L (p_{\text{ref}}/p_m)^n \tag{3}$$

where p_m is the measured motor pressure at the instant when the local burning rate is r_L, r_{LN} is the local burning rate normalized to the reference pressure, p_{ref}. In the above law the pressure index, n, of the propellant was obtained ($n = 0.34$) by conducting separate motor firings at different pressures and measuring the web-average burning rates by the standard method (using web thickness and motor burn time).

In Fig. 4, the ratio of the normalized local burning rate (r_{LN}) to the web-average burning rate normalized to 3.24 MPa (r_{AN}) is plotted as a function of web burnt for the four test firings. An augmentation of ~2–3% in burning rate in the midweb region of the propellant grain is observed for all motors. Significantly, all the tests show a clear pattern, that is, a lower local burning rate in the initial and final portions of the web and a higher local burning rate in the midweb region. The trend is seen to be quite consistent; the same trend is observed in all four BEM tests.

With the use of the measured local burning rates, motor pressures were computed and compared with the measured pressures. Figure 5 shows the comparison for BEM-1. An excellent match

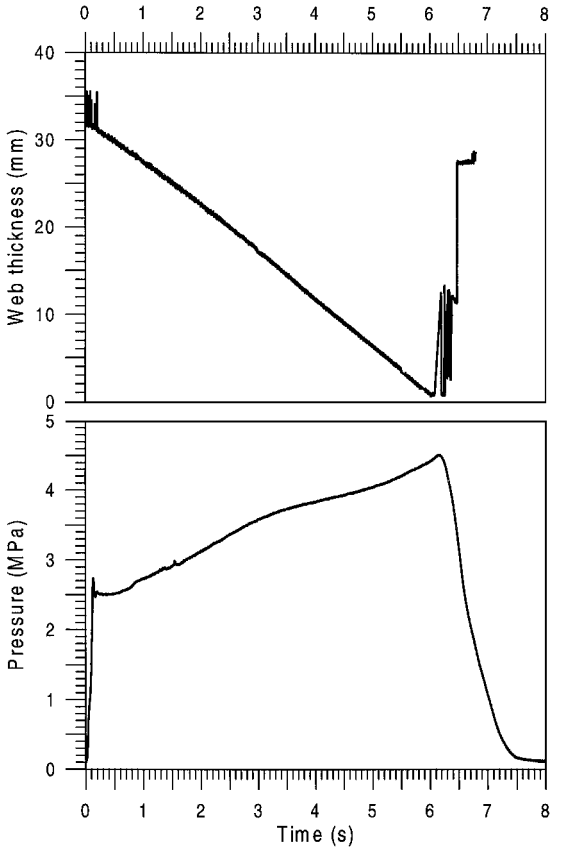

Fig. 3 PIM output (web thickness) and pressure of BEM-1.

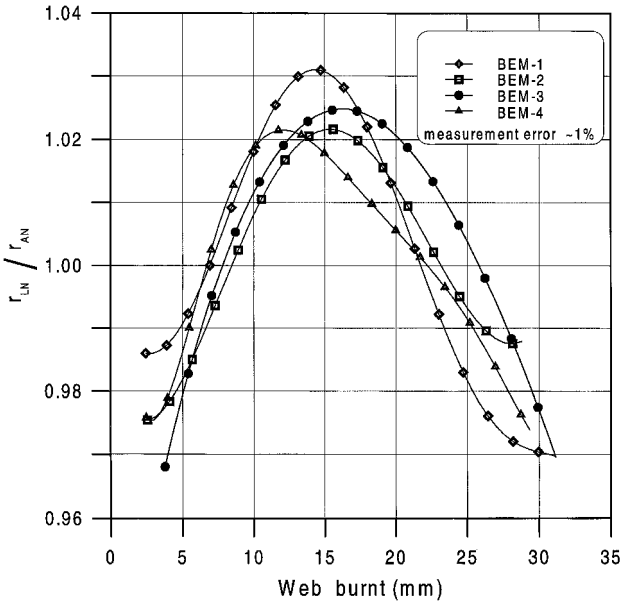

Fig. 4 Variation of local burning rates across the web of the grain.

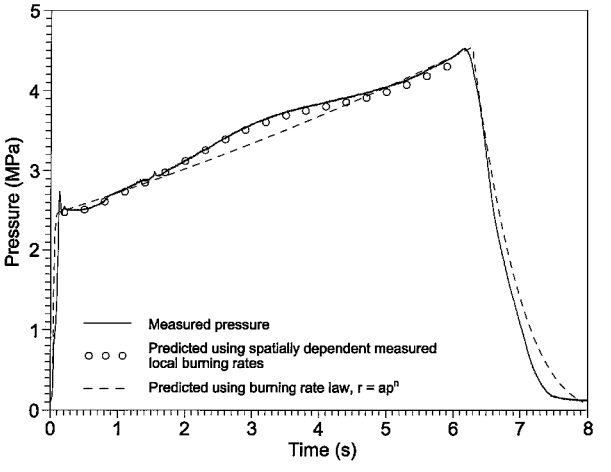

Fig. 5 Comparison of measured pressure with predictions (BEM-1).

of the pressure histories is observed, including the midweb region. Similar results were obtained for the other three motor tests (BEM-2–BEM-4). This indicates the spatial variation of burning rate across the web to be the cause of midweb anomaly. The pressures predicted by the standard ballistic prediction method of using the burning-rate law, $r = ap^n$ (which considers the burning rate to be a function of pressure, but independent of location in the web), are also plotted in the figure. These are lower than the measured pressures in the midweb region. This gap is bridged, and a considerable improvement in prediction is indicated by the use of spatially dependent burning-rate data.

Conclusions

With the use of an ultrasonic pulse-echo technique, a spatial variation of the burning rate across the web has been measured in center-perforated grains of Al-AP-HTPB composite, solid propellant motors. The burning rate is measured to be higher in the midweb region and lower toward the wall of the motor case and the motor port. The motor pressures computed from the measured local burning rates at different instants of time compare very well with the measured pressure–time history of the motor. Direct evidence is given that the main cause of midweb anomaly is the spatial variation of burning rate across the web of the propellant grain.

Acknowledgments

The authors are extremely thankful to B. C. Pillai, Group Director, Propulsion Group, for his encouragement and support of this program. Thanks are also extended to various agencies within the Centre who have helped in this program: the Rocket Propellant Plant for case insulation, propellant casting, end inhibition, and assembly of the motors; the Initiators and Igniters Division of the Space Ordnance Group for providing the igniters; and the Rocket Systems Testing Division for carrying out the static tests.

References

[1] Kallmeyer, T. E., and Sayer, L. H., "Differences Between Actual and Predicted Pressure-Time Histories of Solid Rocket Motors," AIAA Paper 82-1094, June 1982.

[2] Beckman, C. W., and Geisler, R. L., "Ballistic Anomaly Trends in Subscale Solid Rocket Motors," AIAA Paper 82-1092, June 1982.

[3] Friedlander, M. P., III, and Jordan, F. W., "Radial Variation of Burning Rate in Centre Perforated Grains," AIAA Paper 84-1442, June 1984.

[4] Heister, S. D., "Ballistics of Solid Rocket Motors with Spatial Burning Rate Variations," *Journal of Propulsion and Power*, Vol. 9, No. 4, 1993, pp. 649–651.

[5] Koury, J. L., "Solid Strand Burn Rate Technique for Predicting Full Scale Motor Performance," Air Force Rocket Propulsion Lab., Rept. TR-73-49, Oct. 1973.

[6] Neilson, A. M., and Miles, W. L., "Space Shuttle Solid Rocket Motor Reproducibility and the Apparent Influence of Propellant Processing Characteristics on Trace Shape," AIAA Paper 89-2310, July 1989.

[7] Veit, P. W., Landuk, L. G., and Svob, G. J., "Experimental Evaluation of As-Processed Propellant Grains," *Journal of Propulsion and Power*, Vol. 1, No. 6, 1985, pp. 494–497.

[8] Korting, P. A. O. G., and Schoyer, H. F. R., "Determination of the Regression Rate in Solid Fuel Ramjet by Means of the Ultrasonic Pulse-Echo Method," *Proceedings of the 23rd National Heat Transfer Conference*, edited by C. K. Law, Y. Jaluria, W. W. Yuen, and K. Miyasaka, American Society of Mechanical Engineers, New York, 1985, HTD-Vol. 45, pp. 347–353.

[9] Dijkstra, F., Korting, P. A. O. G., and van den Berg, R. P., "Ultrasonic Regression Rate Measurement in Solid Fuel Ramjets," AIAA Paper 90-1963, July 1990.

[10] Kuentzmann, P., Demarais, J. C., and Cauty, F., "Mesure de la Vitesse de Combustion des Propergols Solides par Ultrasons," *La Recherche Aerospatiale*, Vol. 1, No. 1, 1979, pp. 55–79.

[11] Traineau, J. C., and Kuentzmann, P., "Ultrasonic Measurements of Solid Propellant Burning Rates in Nozzleless Rocket Motors," *Journal of Propulsion and Power*, Vol. 2, No. 3, 1986, pp. 215–222.

[12] Deepak, D., Jeenu, R., Sridharan, P., and Padmanabhan, M. S., "Determination of Pressure Dependence of Burning Rate in Solid Motors Using Ultrasonic Technique," *Journal of Propulsion and Power*, Vol. 14, No. 3, 1998, pp. 290–294.